SUPPLEMENTARY INFORMATION

An Efficient ICT based Fluorescence Turn-On Dyad for Selective Detection of Fluoride and Carbon dioxide

Rashid Ali, Syed S. Razi, Ramesh C. Gupta, Sushil K. Dwivedi and Arvind Misra*

Department of Chemistry, Faculty of Science, Banaras Hindu University, Varanasi – 221 005 UP INDIA

Corresponding auther: arvindmisra2003@yahoo.com; amisra@bhu.ac.in
Tel: +91-542-6702503; Fax: +91-0542-2368127, 2368175.

Contents

Figure S14: ^{1}H NMR spectrum of **2** upon addition of 1.0 equiv of F^- in DMSO-d_6.

Figure S15: ^{1}H NMR spectrum of **2** upon addition of 2.0 equiv of F^- in DMSO-d_6.

Figure S16: ^{1}H NMR spectrum of **2** upon addition of 3.0 equiv of F^- in DMSO-d_6.

Figure S17: ^{1}H NMR spectrum of **2** upon addition of 5.0 equiv of F^- in DMSO-d_6.

Figure S18: Fluorescence intensity change of **2+F$^-$** system (1 μM, λex = 370 nm) upon bubbling with different concentration of CO_2 gas.

Figure S19: Change in emission spectra of **2** (1 μM) at (a) λ_{ex} = 370 nm (b) λ_{ex} = 405 nm, upon bubbling of 25 mL of different gases (H_2S, SO_2, HCl and CO_2) to the solution of **2**+ F^- in H_2O-DMSO (20%).

Figure S20: ^{1}H NMR spectrum of **3** in DMSO-d_6.

Figure S21: ^{13}C NMR spectrum of **3** in DMSO-d_6.

Figure S22: FT-IR spectrum of **3**.

Figure S23: Mass spectrum of **3**.

General

Materials and Chemicals. All the reagents and solvents were purchased from Sigma-Aldrich Chemical Co. Pvt. Ltd. stored in a desicator under vacuum containing self indicating silica, and used without any further purification. Solvents were purified prior to use. UV-vis absorption spectra were recorded on a Perkin Elmer Lambda-35 UV-vis spectrophotometer using a quartz cuvette (path length = 1cm). Infrared (IR) spectra were recorded in potassium bromide (KBr) on Varian-3100 FT-IR spectrometer. ^{1}H NMR spectra (chemical shifts in δ ppm) were recorded on a JEOL AL 300 FT-NMR (300 MHz) spectrometer, using tetramethylsilane (TMS) as internal standard. Fluorescence spectra were recorded on Varian eclipse Carry spectrofluorometer using a quartz cuvette (path length = 1 cm) at 600 PMT voltage and slit width 5nm/5nm. All the spectroscopic experiments were carried out at room temperature. The stock solution of **2** ($1x10^{-3}$ M) were prepared in DMSO and diluted to obtain 5 μM and 1 μM solution in DMSO for the absorption and fluorescence measurements, respectively. The stock solutions of different anions ($1x10^{-1}$ M) were prepared by dissolving their tetrabutylammonium salt in MeCN. The anion interaction studies were performed by the addition of 140 equiv. of $1x10^{-1}$ M of different anions. The absorption and fluorescence titration experiment were performed by the gradual increase of concentration of F^- (c =$1x10^{-2}$).

Estimation of Quantum Yields. The quantum yields of probe **2** and **2-F$^-$** were estimated with respect to the quinine sulfate (Φ = 0.54) as standard in 0.1M H_2SO_4 solution by secondary methods,[12] using equation (1).

$$\mathbf{Q = Q_R . I/I_R . OD_R/OD . n^2/n^2_R} \qquad \mathbf{(1)}$$

Where Q is the quantum yield, *I* is the integrated intensity, OD is the optical density, and n is the refractive index. The subscript R refers to the reference fluorophore of known quantum yield.

Estimation of Binding Constant. The absorption and fluorescence experimental data were utilized to calculate association constants by Benesi-Hildebrand method[24] (B-H method) employing equations (2) for 1:1 stoichiometries.

$$\mathbf{1/(\mathit{I} - \mathit{I_o}) = 1/(\mathit{I} - \mathit{I_f}) + 1/K(\mathit{I} - \mathit{I_f})[M]} \qquad \mathbf{(2)}$$

Where K is the association constant, I is the absorbance/fluorescence intensity of the free probe **2**, I_o is the observed absorbance/fluorescence intensity of the **2**-$\mathbf{F^-}$ complex, and I_f is the absorbance/fluorescence intensity at saturation level.

Estimation of Limit of detection. The limit of detection (LOD) of **2** for $\mathbf{F^-}$ was estimated by equation (3).

$$\mathbf{LOD} = 3\sigma / m \qquad \mathbf{(3)}$$

Where, σ stands for the standard deviation of blank solution of **2** and m stands for calibration sensitivity toward F^- ions in DMSO solution of **2**.

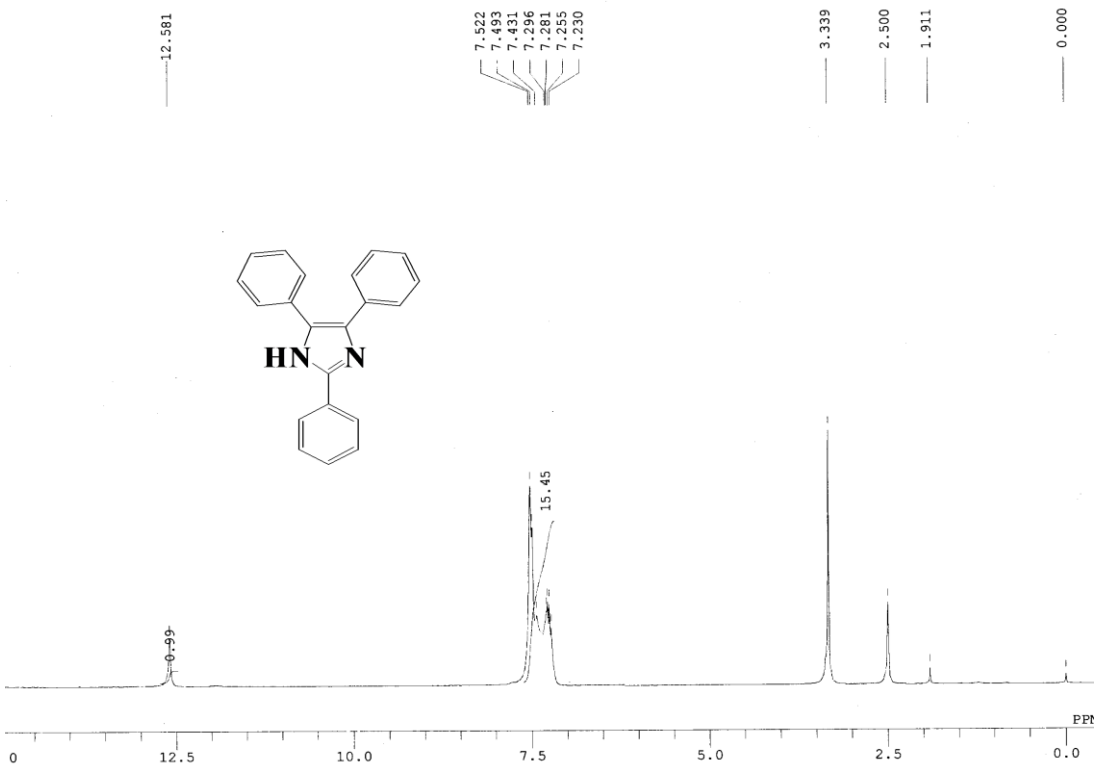

Figure S1: ^{1}H NMR spectrum of **1a** in DMSO-d_6.

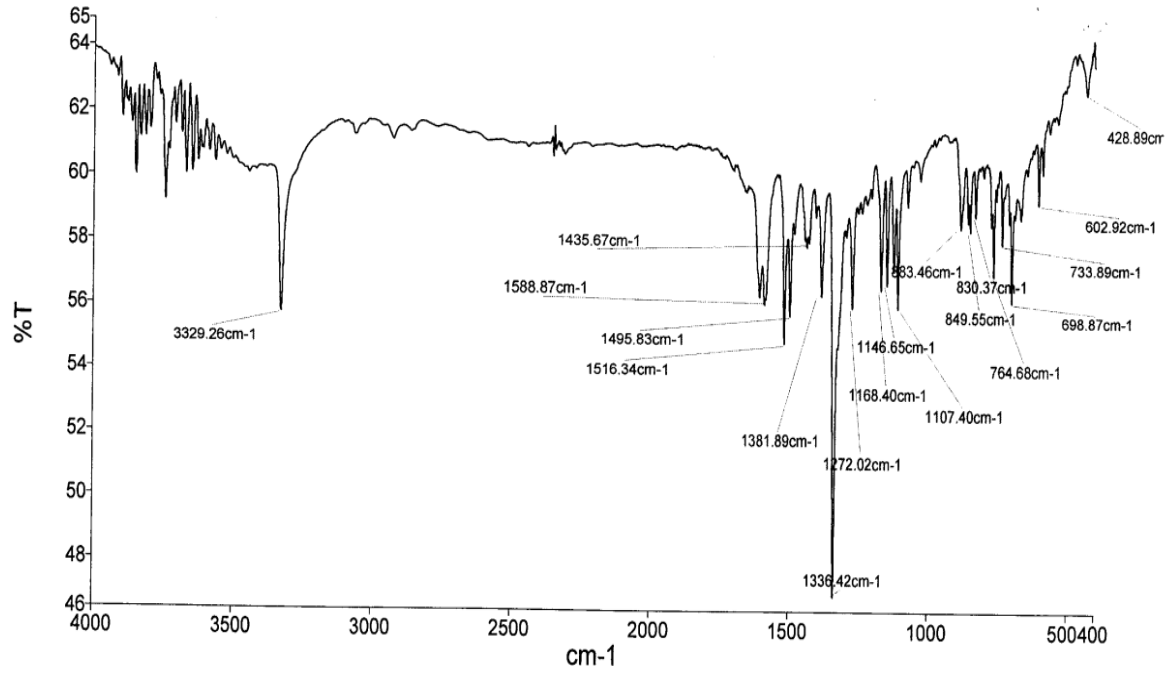

Figure S2: FT-IR spectrum of **1a**.

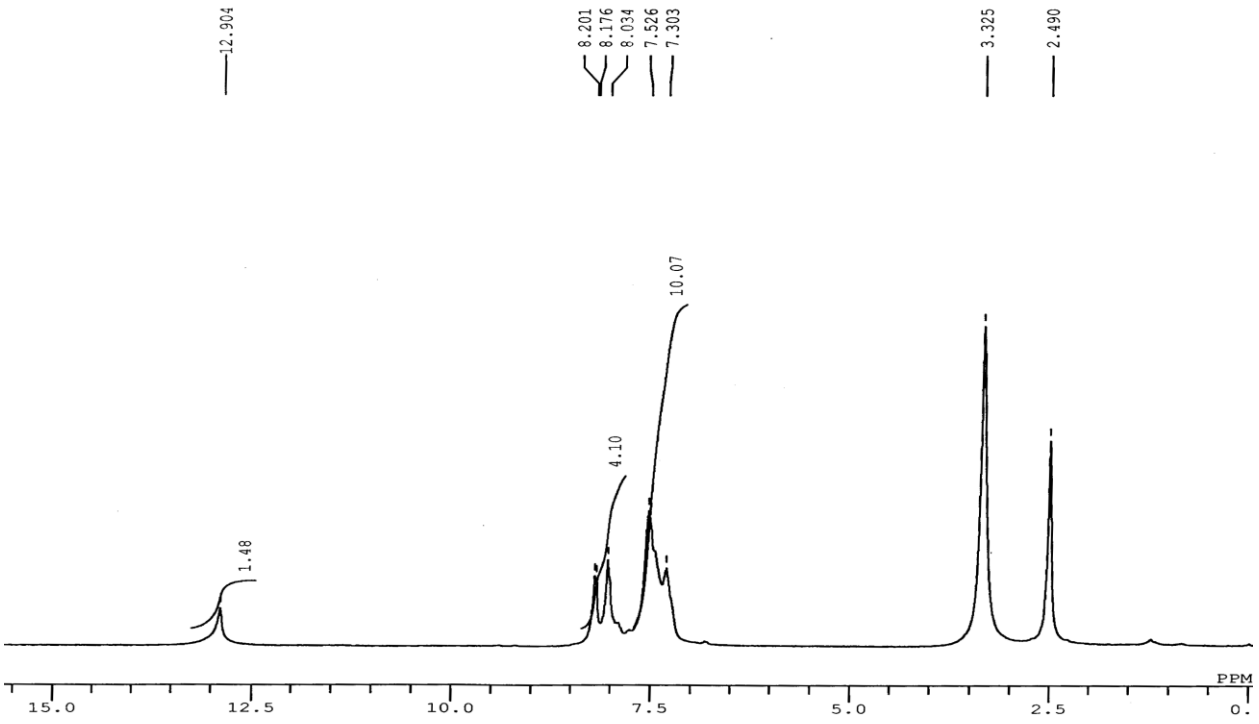

Figure S3: ^{1}H NMR spectrum of **1b** in DMSO-d_6.

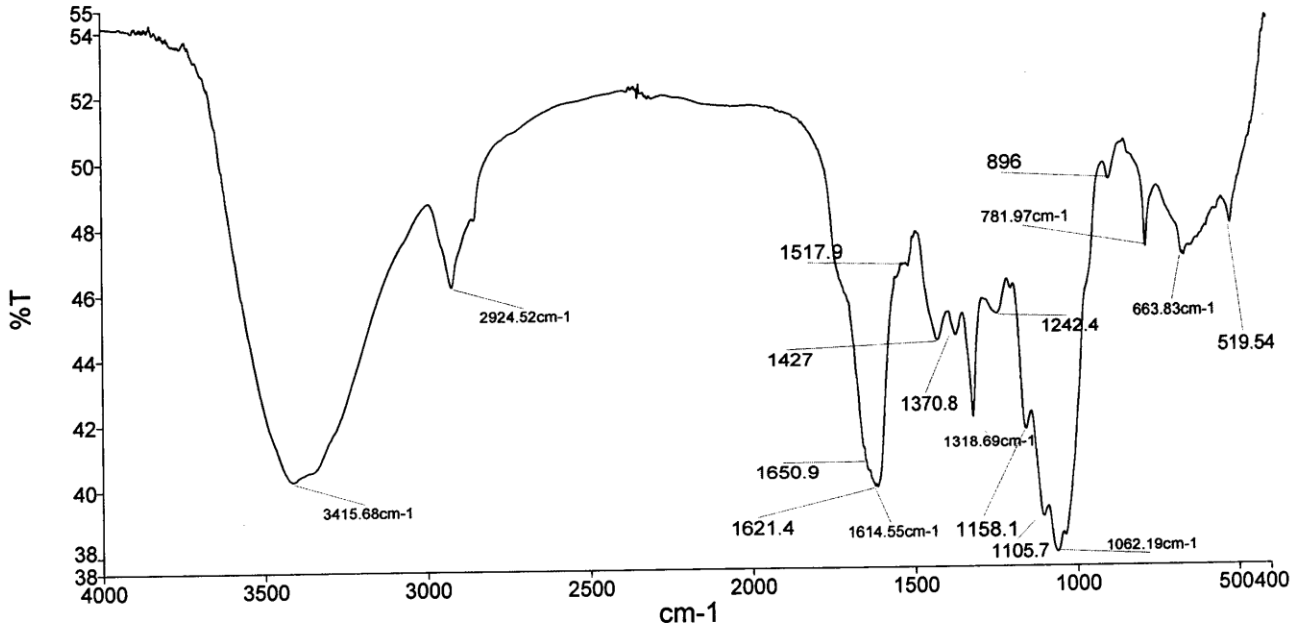

Figure S4: FT-IR spectrum of **1b**.

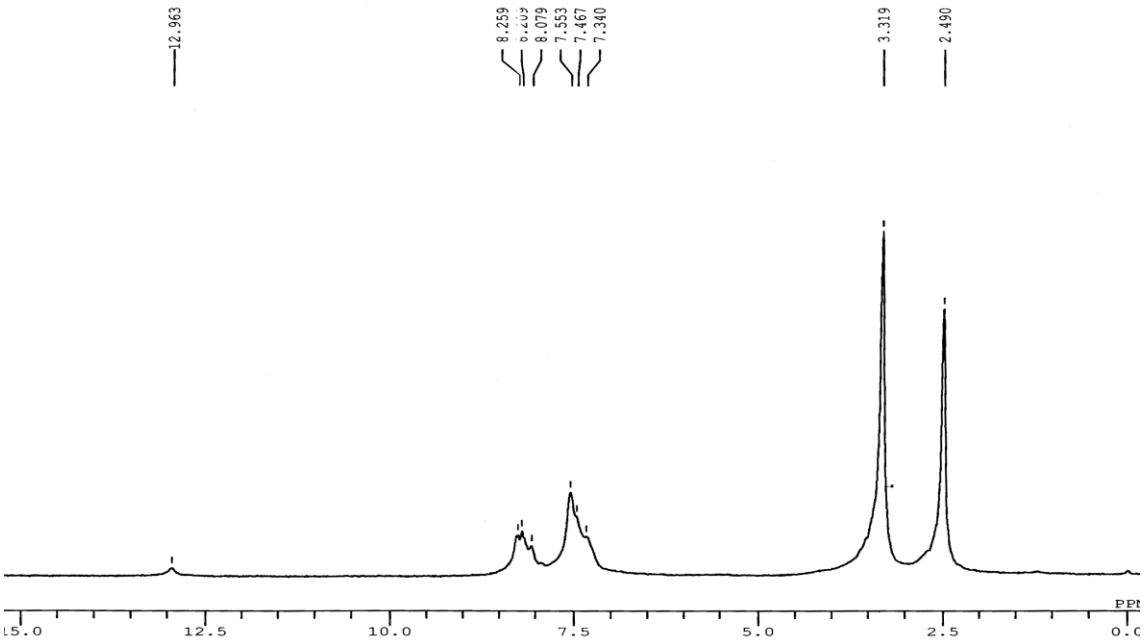

Figure S5: ^{1}H NMR spectrum of **2** in DMSO-d_6.

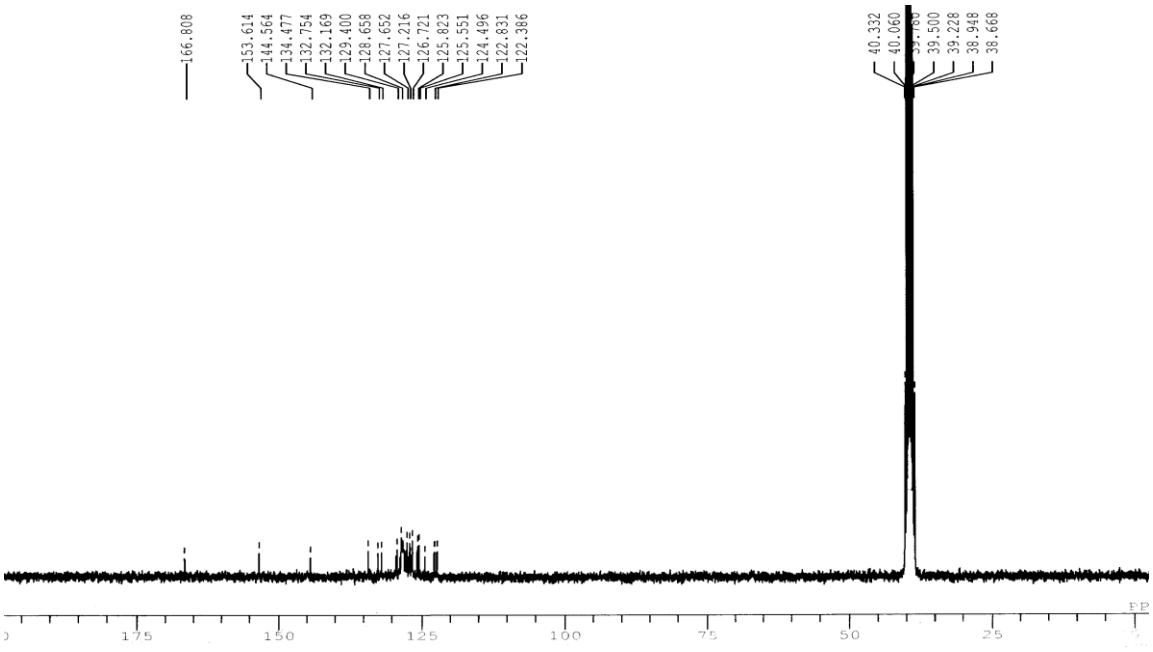

Figure S6: ^{13}C NMR spectrum of **2** in DMSO-d_6.

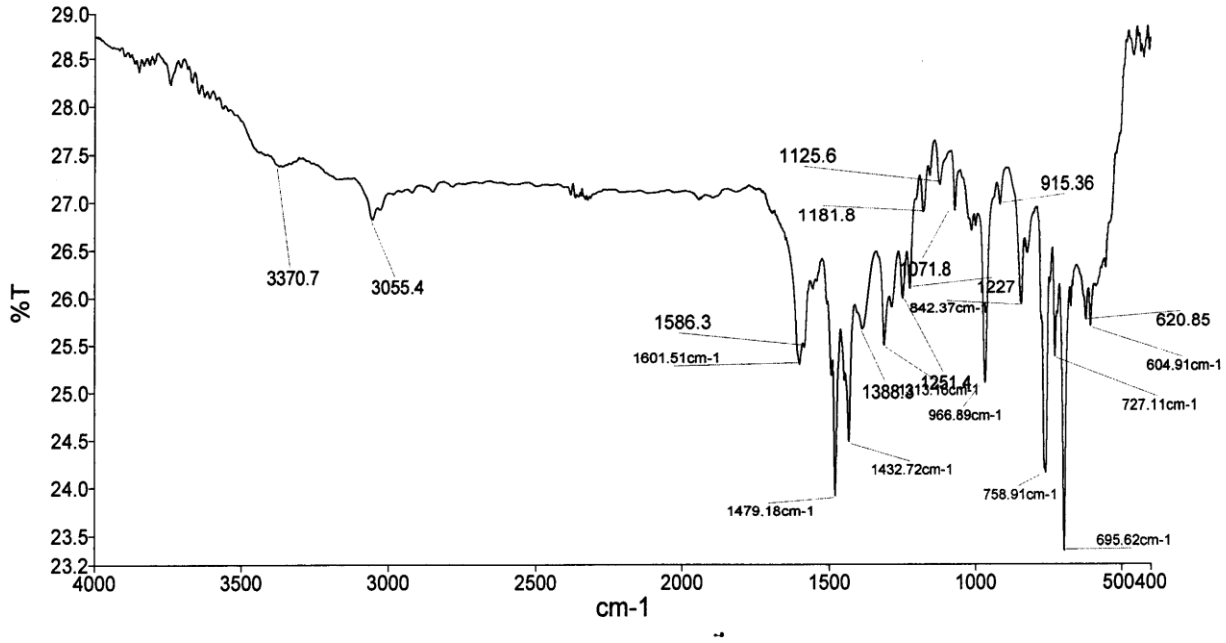

Figure S7: FT-IR spectrum of **2.**

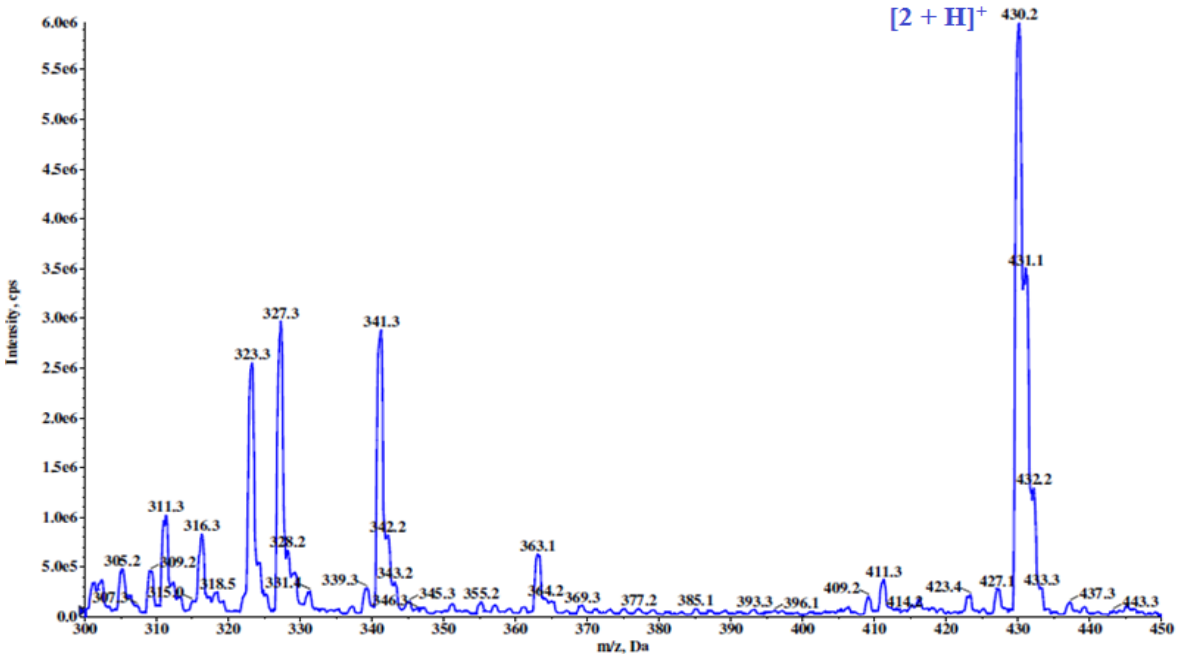

Figure S8: ESI-MS spectrum of **2**.

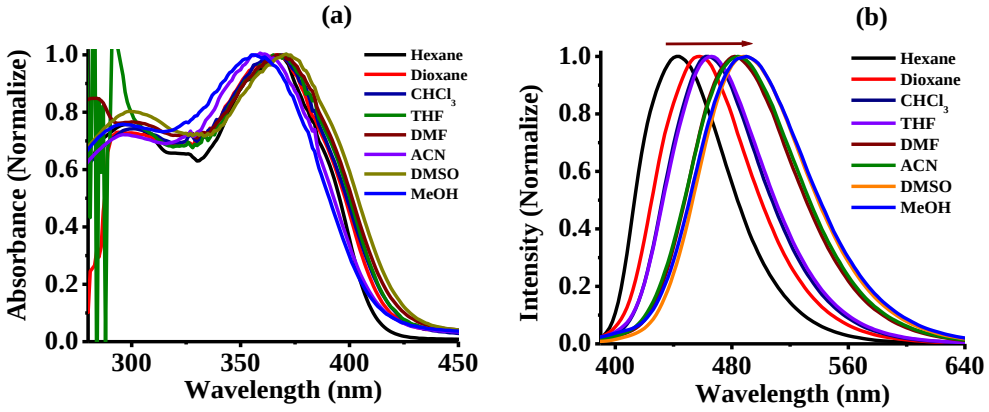

Figure S9: Normalized (a) Absorption and (b) Emission spectra of probe **2** in different solvents.

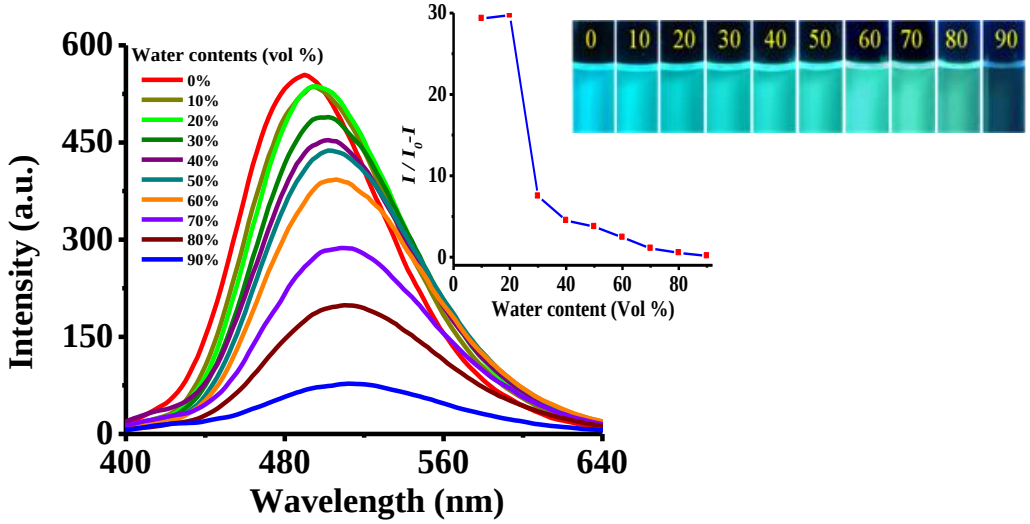

Figure S10: Fluorescence spectra of **2** in DMSO-Water mixtures with different water contents. Inset: the dependence of the fluorescence intensity on the composition of water and the corresponding fluorescence images of **2**.

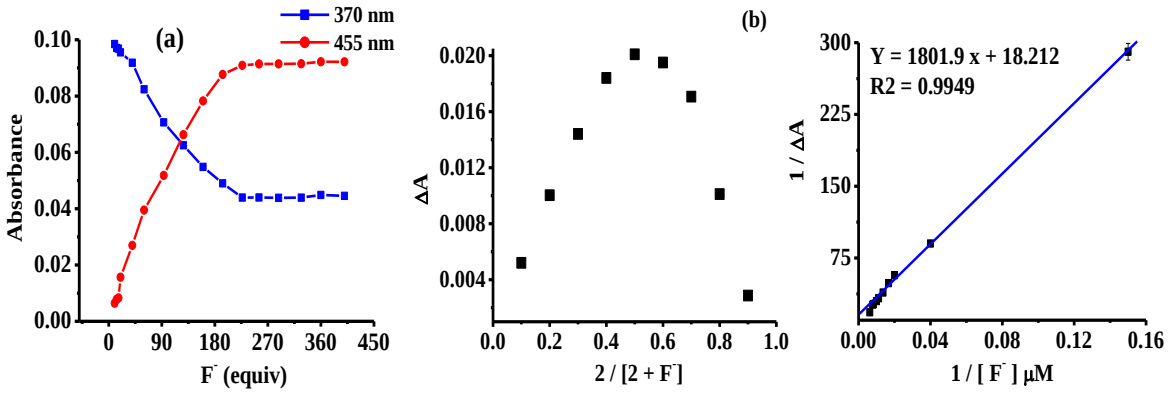

Figure S11: (a) Change in absorption as a function of F^- and (b) Job's plot and Benesi-Hildebrand plots based on absorption spectra.

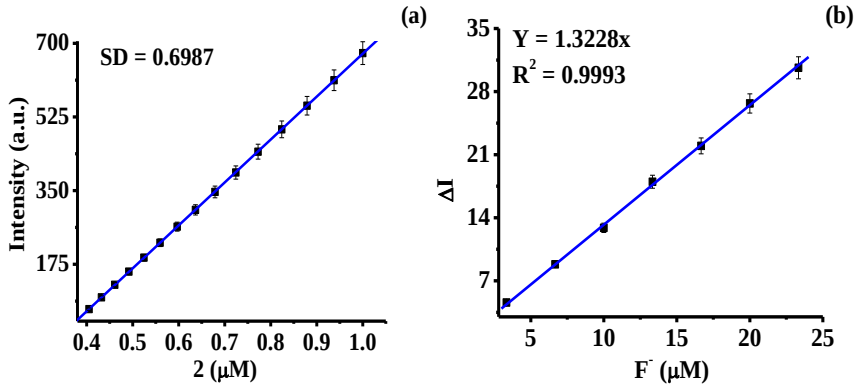

Figure S12: (a) Calibration curve for **2** (b) Calibration sensitivity curve (m) for **2** with F^-. *ΔI* show the change in emission intensity of **2** upon addition of F^-.

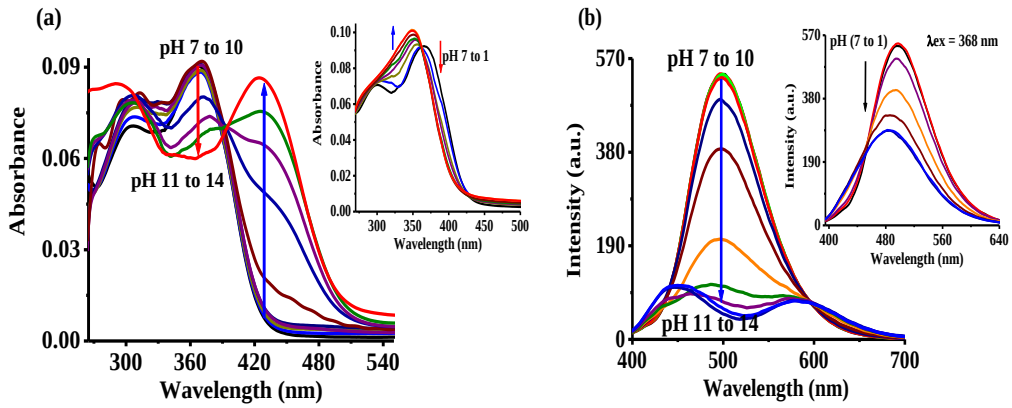

Figure S13: (a) Change in absorption (5μM) and (b) emission (1μM, λ_{ex}=368 nm) spectra of **2** at different pHs in HEPES buffer.

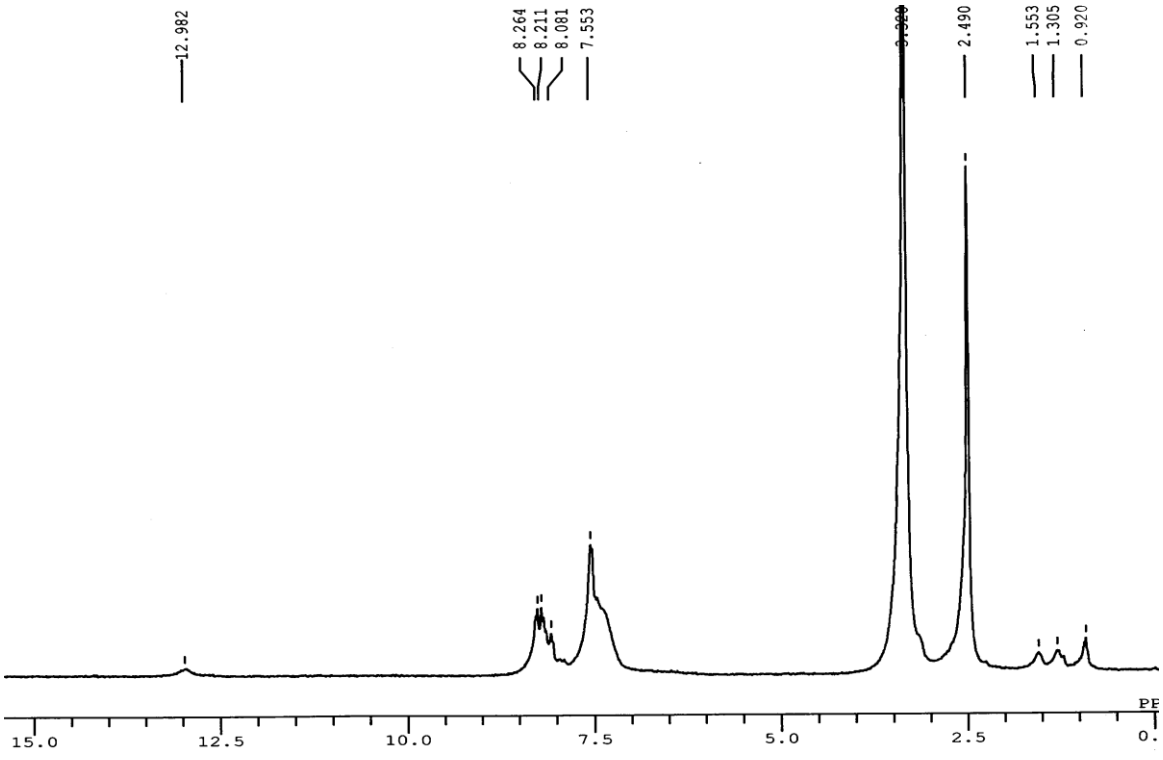

Figure S14: ^{1}H NMR spectrum of **2** upon addition of 1.0 equiv of F^- in DMSO-d_6.

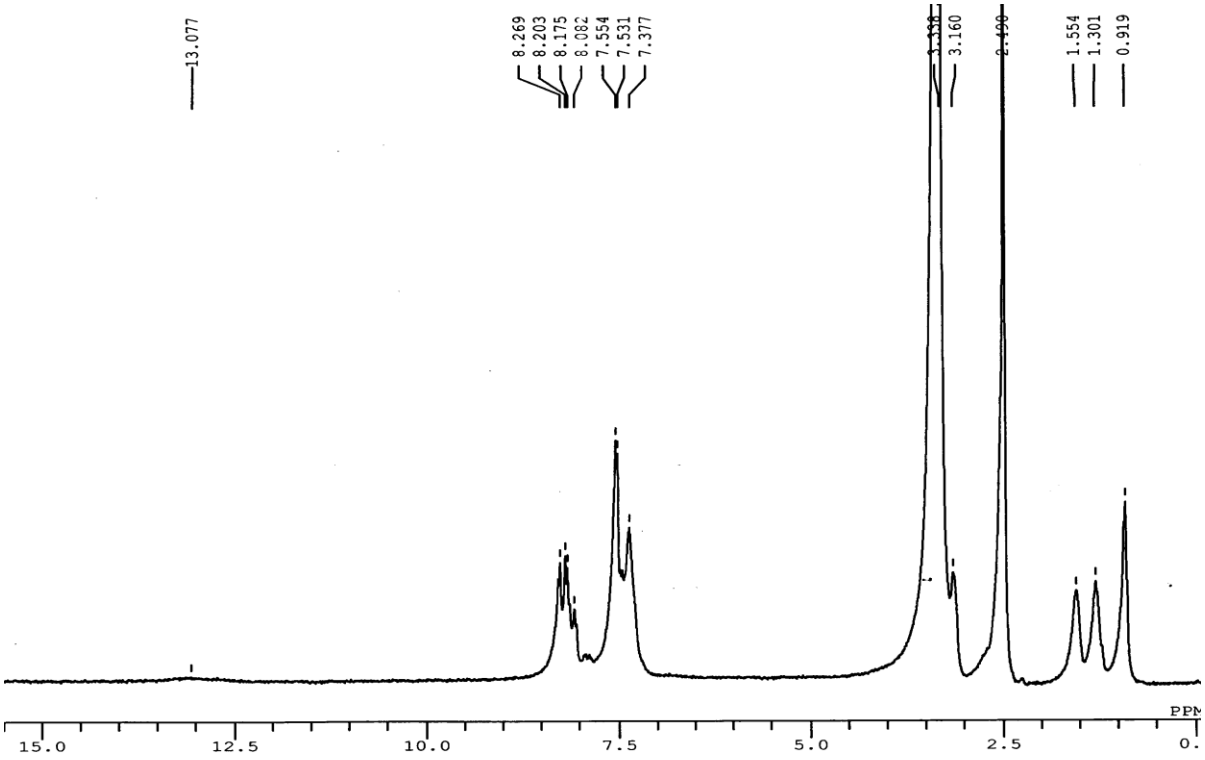

Figure S15: ^{1}H NMR spectrum of **2** upon addition of 2.0 equiv of F^- in DMSO-d_6.

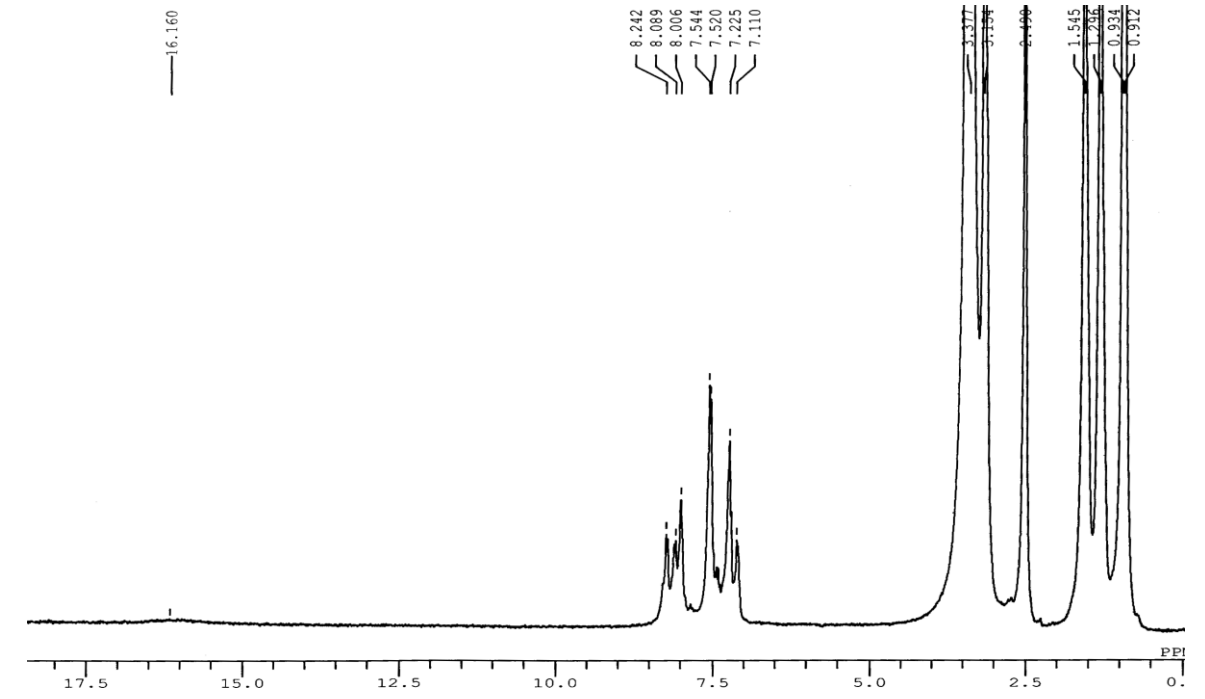

Figure S16: ^{1}H NMR spectrum of **2** upon addition of 3.0 equiv of F^- in DMSO-d_6.

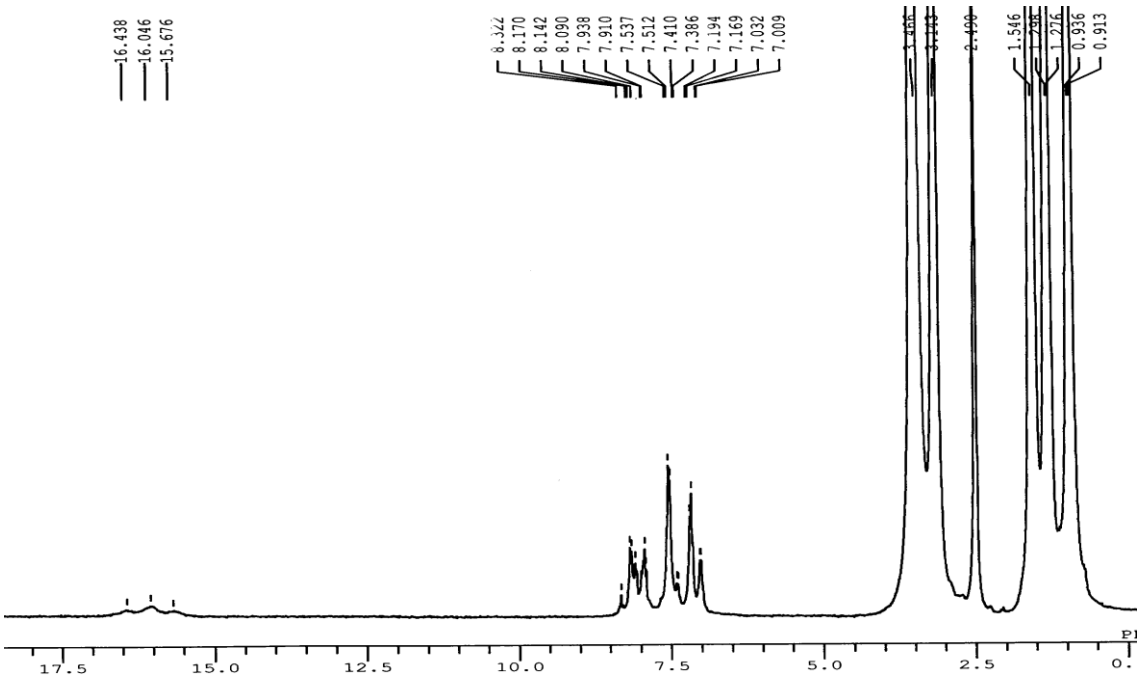

Figure S17: ^{1}H NMR spectrum of **2** upon addition of 5.0 equiv of F^- in DMSO-d_6.

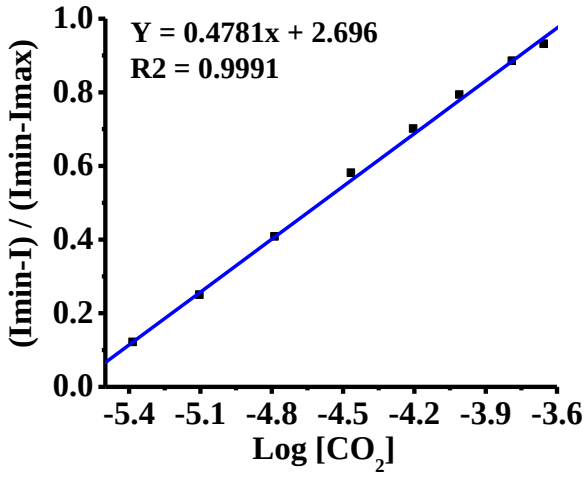

Figure S18: Fluorescence intensity change of **2+F**$^-$ system (1 μM, λex = 370 nm) upon bubbling with different concentration of CO_2 gas.

The detection limit of **2+F**$^-$ system for CO_2 was estimated from plot of normalized fluorescence change of **2+F-** system with CO_2 verses Log [CO_2] using equation (4)[1,2] and found to be 2.29 x 10^{-6} M.

$$\mathbf{10^{\,-[Slope\ /\ Intercept]}} \qquad \mathbf{(4)}$$

1. Shortreed, M.; Kopelman, R.; Kuhn, M.; Hoyland, B. *Anal. Chem.* **1996,** 68, 1414-1418.

2. Kim, M. H.; Jang, H. H.; Yi, S.; Chang S.-K.; Han, M. S. *Chem. Commun.* **2009**, 4838-4840.

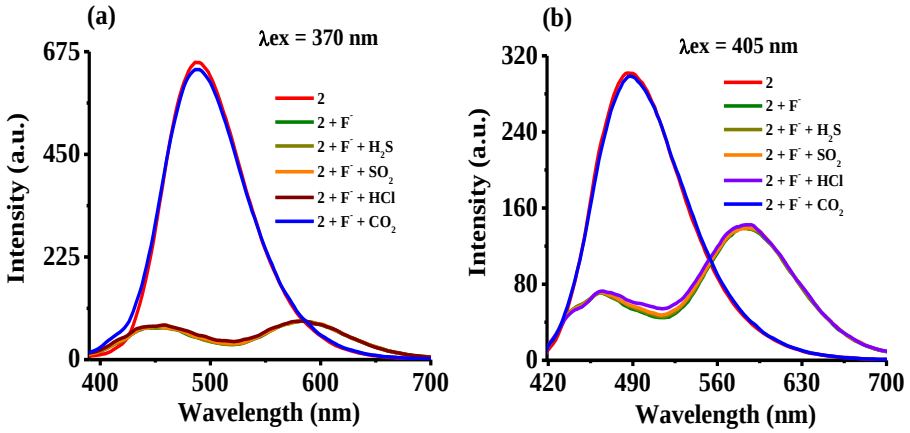

Figure S19: Change in emission spectra of **2** (1 μM) at (a) λ_{ex} = 370 nm (b) λ_{ex} = 405 nm, upon bubbling of 25 mL of different gases (H_2S, SO_2, HCl and CO_2) to the solution of **2**+ F^- in H_2O-DMSO (20%).

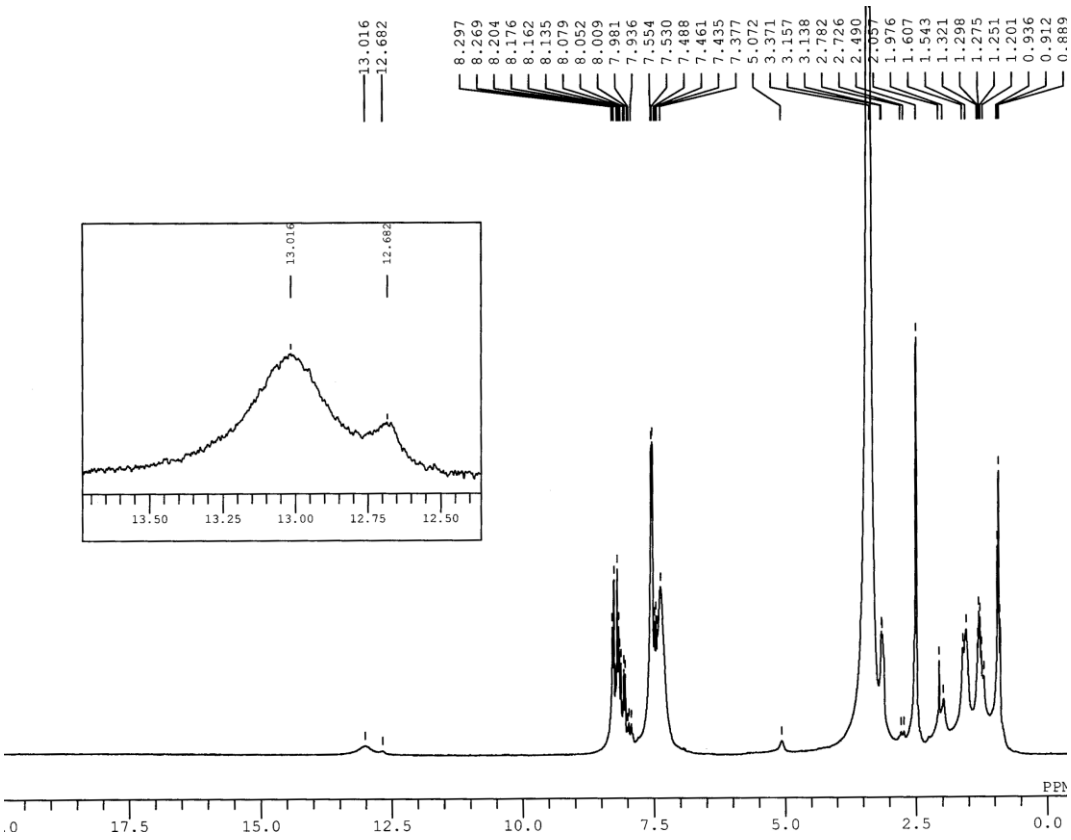

Figure S20: ^{1}H NMR spectrum of **3** in DMSO-d_6.

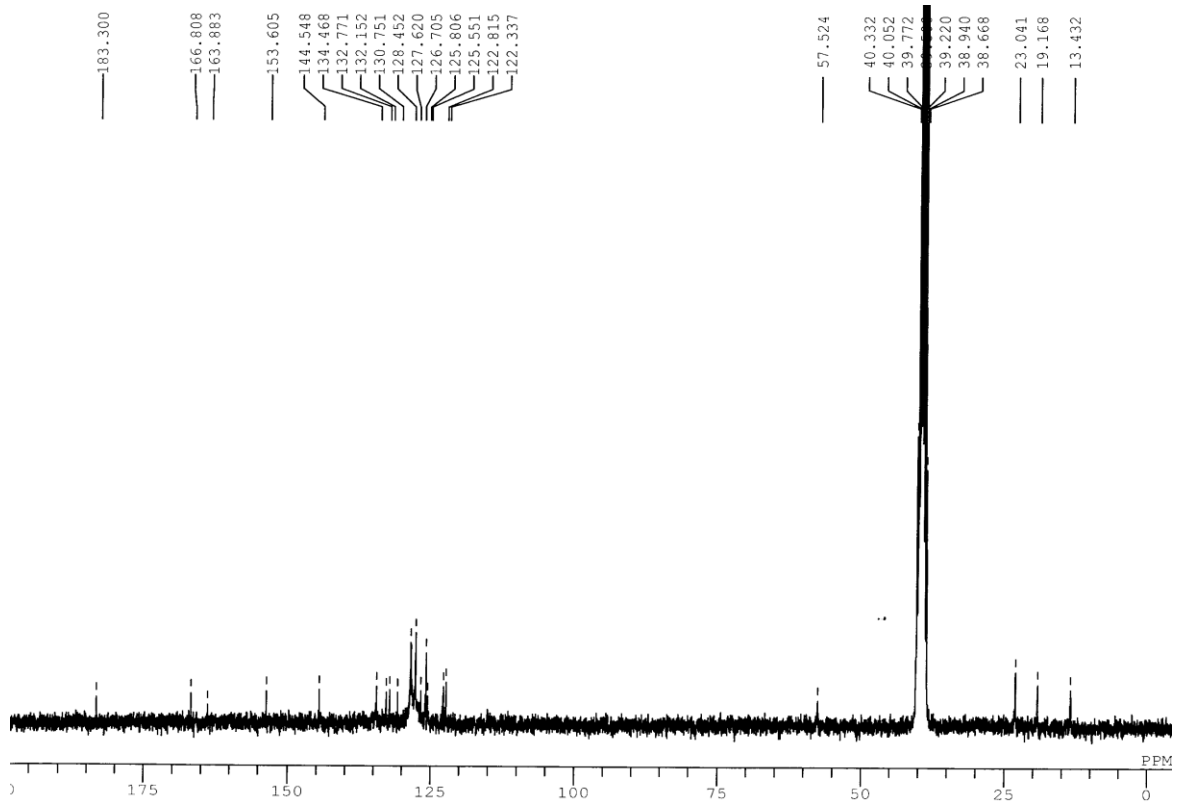

Figure S21: ^{13}C NMR spectrum of **3** in DMSO-d_6.

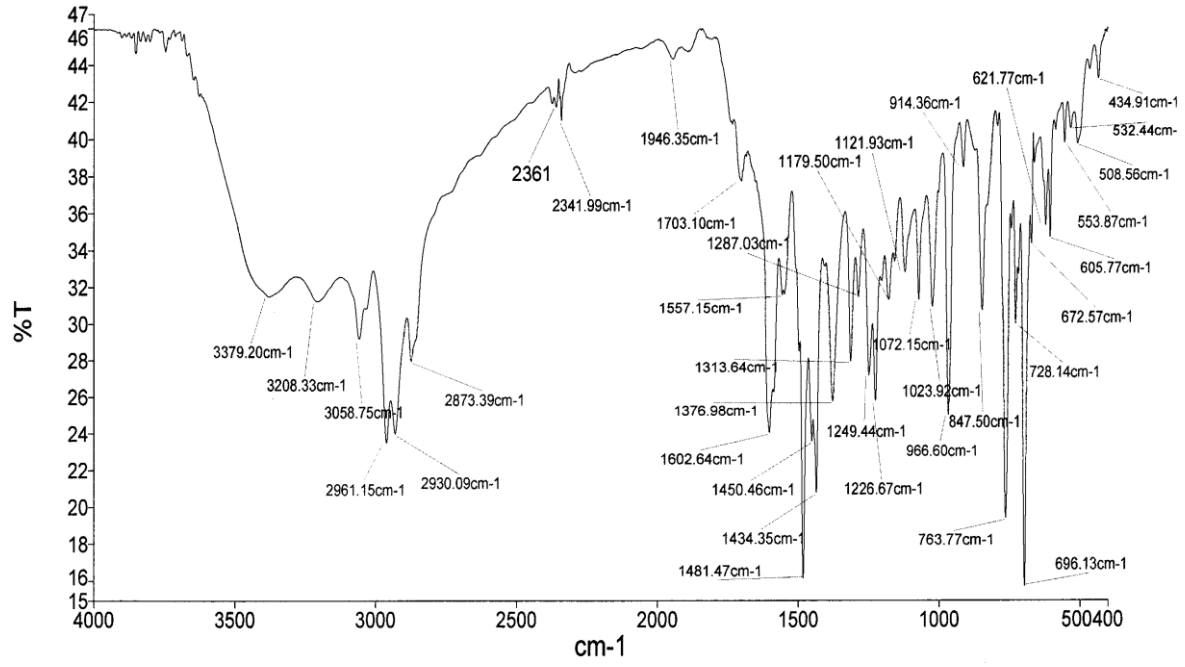

Figure S22: FT-IR spectrum of **3**.

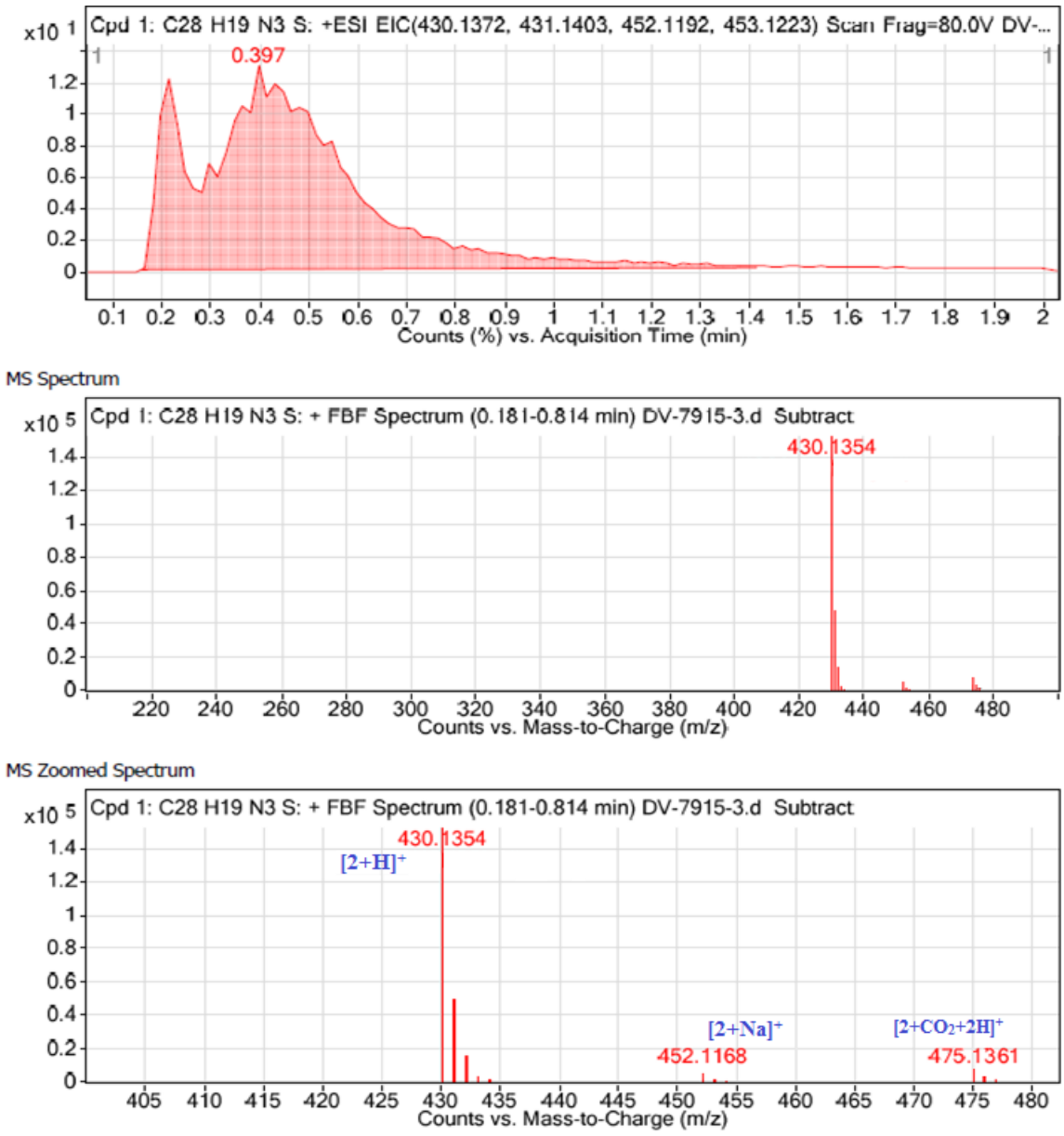

Figure S23: Mass spectrum of **3**.